

## Computational Simulation of the Wind-force on Metal Meshes

Ahmad Sharifian & David R. Buttsworth  
Faculty of Engineering and Surveying  
University of Southern Queensland (USQ)  
Toowoomba, QLD. 4350, Australia

### Abstract

Estimating the drag force on a metal mesh is important if the installed metal mesh area is large and wind speeds are moderate. Such a situation may arise if a metal mesh is used to protect a property from ember attacks in a bushfire prone area. In this work, computational simulations are used to correlate the drag coefficient of a metal mesh in terms of its porosity and the Reynolds number for  $10 \leq Re \leq 1000$ . A benchmarking exercise suggests that the computational simulations may be in error by up to 13 % error for the level of discretization that could be achieved due to computer memory limitations. The drag coefficient correlation we have obtained has a maximum error of only 6.5 % with respect to the results from the simulations.

### Introduction

Metal meshes are used in many applications such as security screens, sport grounds, and roofs of car parks. They are made from different materials with different shapes, sizes and weavings. The wind-force on a metal mesh is particularly important if a large overall size mesh is deployed. However, there does not appear to be any experimental data or reliable analytical equation available to relate the wind-force to the geometry of the metal mesh. An approximate method based on the diameter of the wires used in the metal mesh and the projected area of metal mesh might be used, but in the absence of specific data, a high safety factor would be needed.

This work examines the problem of the wind-force on metal meshes which are used to protect windows and openings of buildings against ember attacks in bushfire prone areas. Australian standard (AS 3959-1999) [1] recommends using metal meshes with an opening of less than 1.8 mm in bushfire prone areas.

Nine metal meshes operating at different Reynolds number are simulated using a commercially-available CFD package and the results are compared with an approximate calculation. Six of the metal meshes that were modelled satisfied Australian standard AS 3959-1999 and the other three meshes were modelled to assist in the deduction of a correlation between wind-force and the metal mesh geometry. All metal meshes were considered to be smooth and to have square metal mesh cells.

The arrangement of the computational elements was achieved using GAMBIT, and the drag force coefficient was calculated using the FLUENT package. Due to computer memory limitations, the boundary layer around the metal mesh was incompletely resolved at the higher Reynolds number conditions and this introduces some errors in determining the drag. These errors are estimated after the physical geometry and the arrangement of the computational elements are introduced in the following sections.

### Modelling

#### Geometry of metal meshes

Metal meshes are manufactured in different shapes and sizes. All metal meshes modelled in this work have a square opening which is the most common shape in use. It is common practice to introduce the geometry of metal mesh as  $m \times n \times d$  where  $m$  and  $n$  are number of metal mesh cells per inch in two orthogonal directions and  $d$  is the diameter of wire in inches. The nine metal meshes modelled in this work are based on 3 different mesh numbers ( $m = n = 10, 16,$  and  $24$ ) each in 3 different wire diameters  $d = 0.0092''$ ,  $0.014''$  and  $0.02''$ . In this work, we also refer to the size or length of a metal mesh cell,  $L = 1/m = 1/n$  if  $L$  is expressed in inches. Metal meshes can be woven in different ways, but only the most common weaving is considered in this work as illustrated in figure 1.

A computational domain with a length and width equal to the metal mesh cell size and a height of at least  $20d$  (consisting in a distance of  $10d$  above and  $10d$  below the mesh location) was defined as illustrated in figure 2. (For the metal mesh  $24 \times 24 \times 0.02''$ , the height of the computational domain was actually  $100d$ .) For the arrangement illustrated in figure 2, the flow inlet is at the bottom of the domain (hidden on the view in figure 2) and the outlet is at the top. The vertical sides of the domain, which pass through the centre of each wire, are planes through which no flow passes.

#### Reynolds numbers

The range of Reynolds numbers investigated in this work is limited to between 10 and 1000. Assuming  $\nu = 1.4607 \times 10^{-5} \text{ m}^2/\text{s}$  (appropriate for air at standard sea level conditions) gives velocities of 225 km/h, 148 km/h and 104 km/h for the three wire diameters  $0.0092''$ ,  $0.014''$  and  $0.02''$  respectively at  $Re = 1000$ . These flow speeds are representative of the highest wind speeds relevant to this work which is motivated by metal mesh protection of structures from bushfires. The wind force at very low wind speeds is not particularly important in this work, but we did want to investigate  $Re$  dependence, so we have selected a minimum Reynolds number of 10.

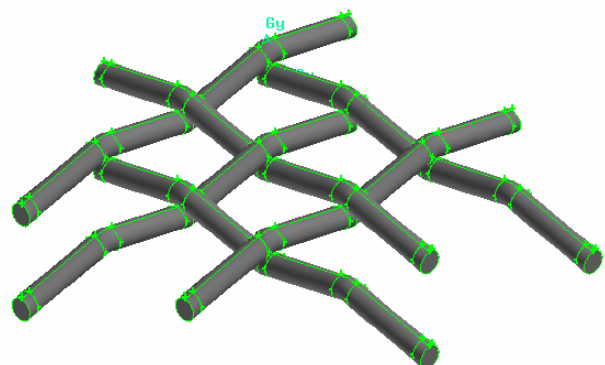


Figure 1 Solid model of the metal mesh prior to defining the computational domain in the case:  $24 \times 24 \times 0.0092''$

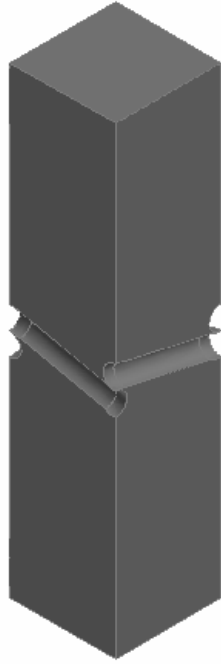


Figure 2 Illustration of the computational domain for the metal mesh case:  $24 \times 24 \times 0.0092''$ . Air enters the domain at the lower horizontal face (hidden) and leaves from the upper horizontal face.

### Elements

The drag force on a metal mesh cannot be simulated reliably without proper modelling of the boundary layer around the metal mesh. In the case of flow around a wire (cylinder), the thickness of the boundary layer is related to the Reynolds number and wire diameter. In a two dimensional wire simulation, the number of elements required for accurate simulation is a function of the Reynolds number, or for a particular flow speed, the number of elements required is a function of the wire diameter.

In the metal mesh case, a three dimensional simulation is required, and the length of wire within the metal mesh cell ( $L$ ) also affects the number of elements required for an accurate simulation. Therefore, at a particular flow speed, the number of required elements increases with the ratio of  $L/d$ . This ratio is related to the mesh number and wire diameter. For example, for the meshes considered in this work, the ratio  $L/d$  reaches a maximum value of 44 for the metal mesh:  $10 \times 10 \times 0.0092''$ , while it has a minimum value of 8 for the metal mesh:  $24 \times 24 \times 0.02''$ .

For the metal mesh  $10 \times 10 \times 0.0092''$ , 73 divisions were produced around the full circumference of the wire. Each edge of the computational domain above and below the wire position was divided into 100 segments and the domain was filled with 3D tetrahedral elements. The total number of elements was approximately 2,500,000 in this case. For the other metal meshes it was possible to increase the number of division around the full circumference of the wires (up to a total of 300 in the case of the metal mesh  $24 \times 24 \times 0.02''$ ) along with increasing the height of the computational domain. Figure 3 shows the elements in the immediate vicinity of the wires for the metal mesh  $24 \times 24 \times 0.0092''$ .

### Boundary conditions

In the Reynolds number range from 10 to 1000, the metal mesh boundary layer should remain laminar [2]. It is also assumed that the air has a uniform speed and enters the domain in the upwards ( $y$ -direction) at the lower entrance; no special conditions are

assumed for the flow at the upper exit which has a minimum distance of  $10d$  from the plane of the metal mesh. The flow medium is air which is assumed to be at atmospheric pressure and room temperature, and is treated as incompressible.

Only one metal mesh cell was modelled. The vertical sides of the computational domain are planes of symmetry plane – see figure 1 – so no air can cross these planes. This suggests the  $C_d$  for a metal mesh should be higher than the  $C_d$  for a single wire of the same diameter due to the effects of flow confinement.

The performance of all nine metal meshes was simulated using at least 7 different Reynolds numbers: 10, 20, 50, 100, 200, 500 and 1000. The total number of elements used in any simulation was between 2,000,000 and 2,500,000 and the run time was about 2-3 hours at low Reynolds number, and to up to 16 hours at the high Reynolds number on a single processor machine speed 1.86 GHz. The combined run time of all the simulations reported here exceeded 400 hours. All metal meshes were assumed to be smooth and no heat transfer was considered. Figure 3 shows the elements immediately adjacent to the wires for the metal mesh  $24 \times 24 \times 0.0092''$ .

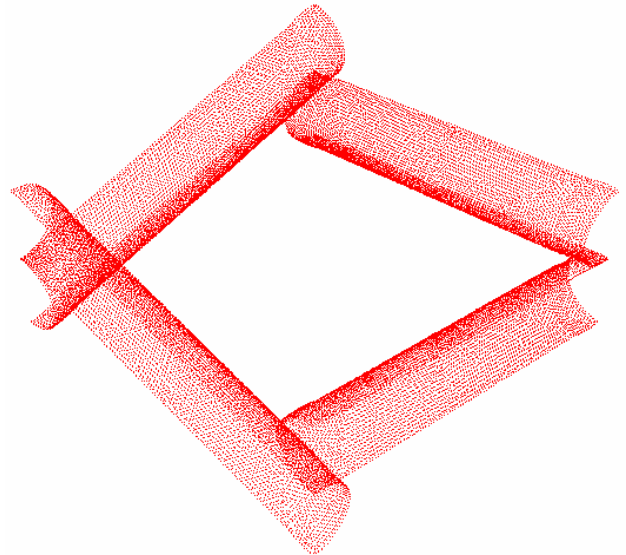


Figure 3 Illustration of the fluid elements around the metal mesh to a depth of one element for the metal mesh:  $24 \times 24 \times 0.0092''$

### Accuracy of modelling – Cylinder Calculations

The drag force can not be calculated reliably if the boundary layer around the wires is not modelled properly. The thickness of the boundary layer around a cylinder depends on the Reynolds number and can be calculated as following [2],

$$\delta \sqrt{\frac{B}{\nu}} = 2.75 \quad (1)$$

where  $\delta$  is the thickness of the velocity boundary layer and  $\nu$  is the kinematic viscosity.  $B$  is the stagnation point velocity gradient which can be estimated using

$$B = 4 \frac{V_\infty}{d} \quad (2)$$

where  $d$  is diameter of the cylinder and  $V_\infty$  is the far field velocity. We can derive the following equation by combining the above equations,

$$\frac{\delta}{d} = 1.375 \text{Re}^{-0.5} \quad (3)$$

Equation 3 indicates that the thickness of the velocity boundary layer decreases with increasing Reynolds number. At the

maximum Reynolds number of 1000, the ratio  $d/\delta$  is 23, so the circumference of the cylinder is about  $73\delta$ .

If we want to accurately simulate the boundary layer and hence model the problem adequately, we would like to have at least 10 elements in the boundary layer and this translates to about 730 elements around the perimeter of wires in the case of approximately square elements.

For the metal mesh  $10 \times 10 \times 0.0092''$ , the length of wire around the perimeter of one metal mesh cell is about 44 times the wire diameter. In the metal mesh simulation, only half of the surface of each wire appears, so the number of elements around this half circumference is  $73\delta/2$ . Assuming the thickness of velocity boundary layer is  $\delta$ , the volume of flow around wire would be  $73\delta/2 \times (44 \times 23\delta) \times \delta = 36938 \delta^3$ . If cubic elements are used and the size of each side is  $\delta/10$ , about 37 millions elements are required to model only the boundary layer and this is beyond our present computational capacity. If instead of requiring 10 elements in the boundary layer, we accept a minimum of only one element at the highest Reynolds number, then the minimum number of required elements required for the boundary layer would be 36938 which is affordable. (A maximum of 2,500,000 elements is possible in the computer we used.) This means we have only 1 element spanning the stagnation point boundary layer at any point for the highest Re condition and hence assessing the accuracy of the simulation becomes an important aspect of our work.

To estimate the errors associated with this rather coarse level of discretisation, cylinder flows are simulated and the results are compared with the well accepted experimental drag coefficient results for a cylinder. The modelling is 2 dimensional and the results are compared with a correlation given by [3] as

$$C_{d,cyl} = \frac{6.8}{Re^{0.89}} + \frac{1.96}{Re^{0.5}} - \frac{1}{\frac{1}{4 \times 10^{-4} Re} + \frac{Re}{1.1 \times 10^{-3}}} + 1.18 \quad (4)$$

In all cases, the discretization is fixed such that we have only one element spanning the stagnation point boundary layer for the highest Re condition. The arrangement of elements in the vicinity of the cylinder is illustrated in figure 4, and in our chosen coordinate system, the flow direction is upwards, entering the domain at the lower edge. Simulations were performed with different heights and widths of the computational domain, and results are summarised in table 1.

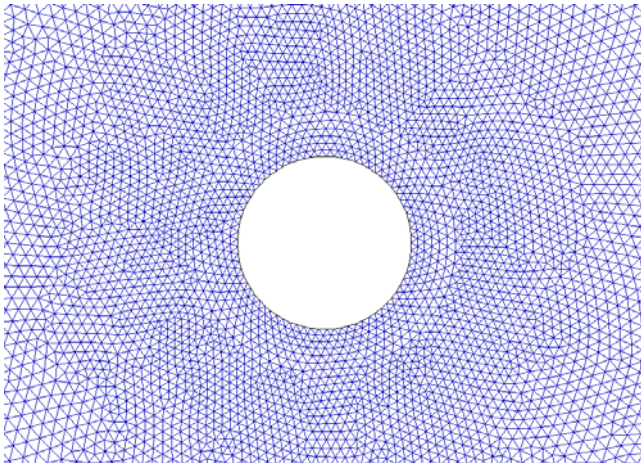


Figure 4 Illustration of element density in the simulation of a single wire perpendicular to the flow

Simulations were performed at the extremes of our Reynolds numbers. The first two columns of Table 1 show that the simulation can give reasonable results with a maximum error of 6%. In the case of  $Re = 10$ , the size of elements near the cylinder is about 10% of the thickness of the stagnation point boundary layer and so this simulation was expected to have less error than the  $Re = 1000$  case, but this did not occur – both cases have an error of 6%. The reason for this may be related to inaccuracy in the reference equation. However, the thickness of velocity boundary layer at  $Re = 10$  is much greater than the thickness at  $Re = 1000$  so another possible reason may be related to the flow restrictions imposed by the finite computational domain. While the effects of domain size in the transverse direction are relevant to the discussion of single wire (cylinder) simulations, they are not particularly important in the metal mesh simulation work. Flow restriction in the transverse direction is an essential physical feature of metal mesh operation.

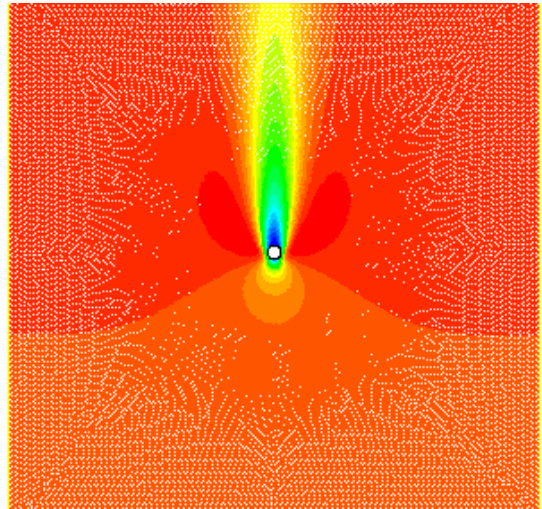


Figure 5 Illustration of the simulated flow around the cylinder at  $Re = 10$ . (Colouring is according to the y-component of velocity.)

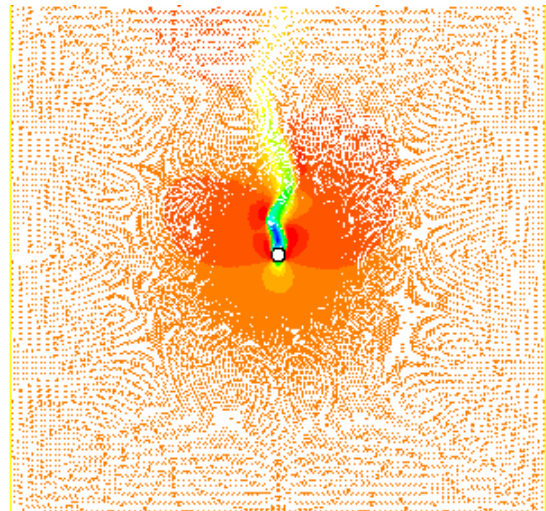


Figure 6 Illustration of the simulated flow around the cylinder at  $Re = 1000$ . (Colouring is according to the y-component of velocity.)

In the second two columns of table 1 the total height of the computational domain (the size of the domain in the streamwise direction) was reduced to the  $20d$ . This modification does not have any effect on  $C_d$  for the case  $Re = 1000$ , but it increases the difference between the simulation result and the cylinder correlation (equation 4) in the case  $Re = 10$ . Hence we conclude that the streamwise size of the domain affects results in the

lowest Reynolds number case if streamwise domain size is  $20d$ . For the metal mesh case  $10 \times 10 \times 0.0092''$ , the height of the domain was  $20d$  due to computer memory limitations and so an error up to 13% is expected.

The last two columns of table 1 provide results for the cylinder simulated using a domain consistent with the three dimensional domain used in the case of the metal mesh  $10 \times 10 \times 0.0092''$ . At both Reynolds numbers, the simulated  $C_d$  value increases due to the decrease in the transverse size of the domain which causes a flow restriction effect, increasing the flow speed past the wire and hence increasing the drag.

domain	height	100d		100d		10.87d	
	width	100d	20d	100d	20d	100d	20d
Re	10	1000	10	1000	10	1000	1000
$C_d$ (simulations)	2.84	0.90	3.03	0.90	3.35	0.93	
$C_{d,cvt}$	2.67	0.96	2.67	0.96	2.67	0.96	
difference (%)	6%	6%	13%	6%	25%	3%	

Table 1 Results on the accuracy of the simulations of a single cylindrical wire in cross flow

### Results and Discussion

Drag coefficient results from all of the metal mesh simulations are presented in table 2. Representative results from the simulations of the metal meshes are presented in figures 7 to 9. The Reynolds numbers in these figures is based on the diameter of the wires in the metal mesh. In this work, the drag coefficient of the metal meshes is defined by taking the flow speed well upstream of the metal mesh (at the entrance to the computational domain), and the reference area as the cross sectional area of one metal mesh cell. (Using the total cross sectional area rather than the projected area of the wires in the metal mesh is convenient for later design work where the aerodynamic force on a particular installed area is required.)

mesh		Re						
$m$	$d$ (")	10	20	50	100	200	500	1000
10	0.0092	0.7629	0.5438	0.3763	0.3021	0.2552	0.2232	0.2079
16	0.0092	1.5141	1.0620	0.7271	0.5832	0.4948	0.4313	0.3978
24	0.0092	3.2151	2.2235	1.5910	1.2420	1.0048	0.8414	0.7378
10	0.0140	1.5088	1.0314	0.6916	0.5505	0.4664	0.3851	0.3480
16	0.0140	3.3152	2.2868	1.5476	1.2383	1.0367	0.8489	0.7614
24	0.0140	8.7704	6.0119	4.0809	3.2508	2.6837	2.1592	1.8658
10	0.0200	2.7737	1.8440	1.2417	0.9898	0.8265	0.6920	0.6143
16	0.0200	7.6868	--*	--*	--*	--*	--*	1.6443
24	0.0200	29.314	19.743	12.921	9.851	7.8331	6.2140	5.1574

\* Simulations for this case were not performed at precisely the given Reynolds numbers. However the following results were obtained:  $(Re, C_d) = (14.286, 6.2285), (28.571, 4.4394), (71.429, 3.1464), (142.86, 2.5670), (285.71, 2.1607)$

Table 2 Coefficient of drag simulation results for all of the metal mesh simulations

Figures 7 to 9 indicate that  $C_d$  is largest at the low Reynolds number and sharply decreases with increasing Reynolds number, but at higher Reynolds numbers (say around 200), the change of the  $C_d$  with  $Re$  is relatively small and reaches an almost constant value up to the highest Reynolds number studied in this work ( $Re = 1000$ ). This behaviour is very similar to the  $C_d$  for flow around a cylinder and is an expected result given the metal mesh is constructed using woven wires. The result implies that the nodes of the weaving pattern do not dramatically alter the global fluid mechanics.

In figures 7 to 9, an approximation for the metal mesh drag coefficient,  $C_{da}$  is also included. This approximation was obtained from equation 4. In effect, we determine the drag force on a single wire of the same diameter as the metal mesh wire, supposing this single wire is exposed to an unconstrained flow of the same speed seen well upstream of the metal mesh. The

length of wire in this single wire approximation was taken as that required for a reference area equal to the projected (solid) metal mesh area. The single wire drag coefficient approximation ( $C_{da}$ ) was then obtained by normalising the drag force using the cross sectional area of a single metal mesh cell, so that results are directly comparable to the simulated metal mesh results ( $C_d$ ).

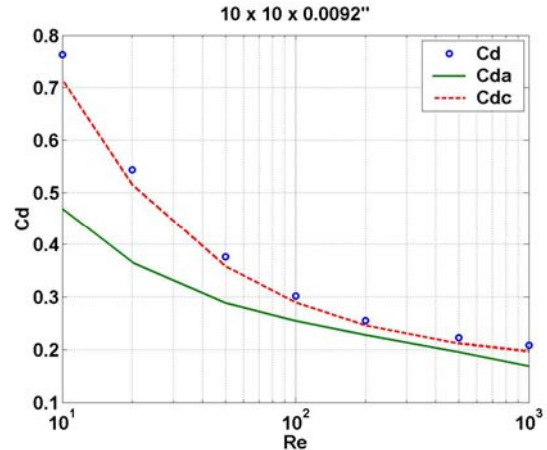


Figure 7 Comparison of drag coefficient from the simulations ( $C_d$ ), the approximate approach ( $C_{da}$ ), and the proposed correlation ( $C_{dc}$ ) for the mesh:  $10 \times 10 \times 0.0092''$ .

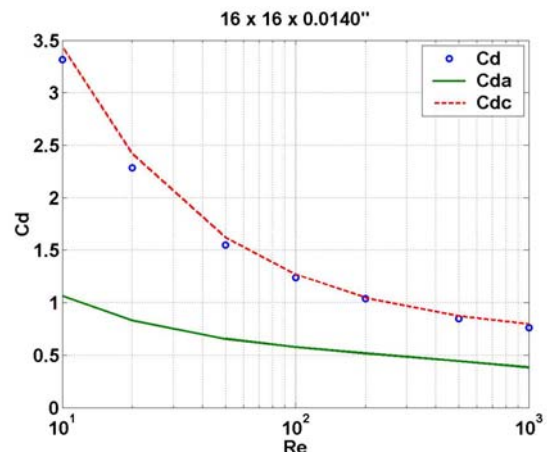


Figure 8 Comparison of drag coefficient from the simulations ( $C_d$ ), the approximate approach ( $C_{da}$ ), and the proposed correlation ( $C_{dc}$ ) for the mesh:  $16 \times 16 \times 0.0140''$ .

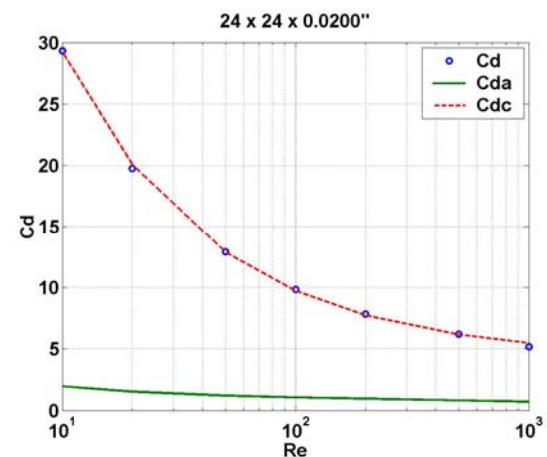


Figure 9 Comparison of drag coefficient from the simulations ( $C_d$ ), the approximate approach ( $C_{da}$ ), and the proposed correlation ( $C_{dc}$ ) for the mesh:  $24 \times 24 \times 0.0200''$ .

From figures 7 to 9, it can be seen that the shape of the graph for  $C_{da}$  is similar to that of  $C_d$  for all metal meshes but the values of

$C_{da}$  are significantly smaller. This is an expected result that reflects the constrained nature of the flow through the metal meshes. These figures also show that the ratio  $C_d / C_{da}$  is greater at lower Reynolds numbers. For example, for the metal mesh  $10 \times 10 \times 0.0092''$ , the ratio  $C_d / C_{da}$  is about 1.6 at a  $Re = 10$  but decreases to 1.2 at  $Re = 1000$ . For metal mesh  $24 \times 24 \times 0.0092''$ , which has the same wire diameter but a smaller opening, the ratio  $C_d / C_{da}$  is about 2.7 at  $Re = 10$  and decreases to about 1.7 at  $Re = 1000$ . This effect arises due to the thickness of boundary layer which increases when Reynolds number decreases (equation 3). Increasing the displacement thickness of the boundary layer has a similar effect to decreasing the width of the passage.

Dimensional analysis indicates that the wire diameter  $d$  relative to the metal mesh cell size  $L$  will probably be an important parameter. The ratio of wire diameter and metal mesh cell length can be embodied in the metal mesh porosity which is the ratio of open area to total area which is therefore given by

$$p = \frac{(L-d)^2}{L^2} = \left(1 - \frac{d}{L}\right)^2 \quad (5)$$

The simulations confirm that porosity  $p$  is an appropriate nondimensional variable. For example, consider  $C_d$  results from the two metal meshes:  $16 \times 16 \times 0.0092''$  and  $10 \times 10 \times 0.014''$  (table 2). At  $Re = 10$ ,  $C_d = 1.5141$  and  $1.5088$  for the  $16 \times 16$  and  $10 \times 10$  metal meshes respectively. These two metal meshes have different cell sizes and diameters but have an almost identical porosity (72.73% and 73.96% respectively).

Based on results presented in table 2, the following equation that correlated  $C_d$  to  $Re$  and  $p$  is proposed,

$$C_{dc} = -0.491 + \frac{0.47}{p^{1.773}} - \frac{7.49}{Re^{0.661}} + \frac{6.475}{p^{2.244} Re^{0.661}} \quad (6)$$

for the ranges  $10 \leq Re \leq 1000$  and  $0.27 \leq p \leq 0.82$ . The above correlation has a maximum error of about 6.5 % with respect to the simulation results.

If equation 6 is used to estimate the total drag force on a metal mesh in an installed configuration, due consideration should be

given to flow effects at the edges of the mesh. For example, at a free edge of the metal mesh, a lower drag force per unit area would be expected due to deflection of the upstream flow away from the mesh. Conversely, a higher drag force may be experience in the vicinity of a mesh edge that is secured to a solid surface if the surface channels the air flow towards the mesh.

## Conclusion

Nine smooth square metal meshes with different diameters and wire spacing were modelled and the drag coefficients were determined through computational simulation at Reynolds number from 10 to 1000. The metal meshes were assumed to be at the same temperature as the flowing air and no heat transfer was considered.

The magnitude of likely errors associated with the finite level of discretization in the three dimensional simulations was estimated by comparing results for a circular cylinder at an equivalent level of discretization with accepted experimental data. It was shown that provided the maximum radial dimension of computational elements adjacent to the cylinder did not exceed the thickness of the cylinder's velocity boundary layer, the cylinder drag was simulated with a maximum error of 13%.

For the three dimensional metal mesh cases considered in this work, it was found that the drag coefficient is a function of the porosity of mesh and the Reynolds number. Based on this result, a correlation for the drag coefficient with a maximum error of 6.5% respect to the simulated results is proposed.

## References

- [1] Standards Australia International, "construction of buildings in bushfire-prone areas, AS 3959-1999", *Standards Australia* (1999), Sydney, Australia.
- [2] White, F.M., *Viscous fluid flow*, 1974, McGraw-Hill, USA.
- [3] Sucker,D & Brauer, H., "Fluiddynamik bei quer angeströmten Zylindern", *Wärme-undstoffübertragung* 8, 1975, pp149-158, Springer-Verlag.